ELSEVIER

Overexpression of Smad2 in Tgf-β3-null mutant mice rescues cleft palate

Xiao-Mei Cui, Nobuyuki Shiomi, Jucheng Chen, Takashi Saito, Tadashi Yamamoto,
Yoshihiro Ito, Pablo Bringas, Yang Chai, Charles F. Shuler*

Center for Craniofacial Molecular Biology, School of Dentistry, University of Southern California, 2250 Alcazar Street, CSA 103,
Los Angeles, CA 90033, USA

Abstract

Transforming growth factor (TGF)-β3 is an important contributor to the regulation of medial edge epithelium (MEE) disappearance during palatal fusion. SMAD2 phosphorylation in the MEE has been shown to be directly regulated by TGF-β3. No phospho-SMAD2 was identified in the MEE in Tgf-β3-null mutant mice (Tgf-β3$^{-/-}$), which was correlated with the persistence of the MEE and failure of palatal fusion. In the present study, the cleft palate phenotype in Tgf-β3$^{-/-}$ mice was rescued by overexpression of a Smad2 transgene in Keratin 14-synthesizing MEE cells following mating Tgf-β3 heterozygous mice with Keratin 14 promoter directed Smad2 transgenic mice (K14-Smad2). Success of the rescue could be attributed to the elevated phospho-SMAD2 level in the MEE, demonstrated by two indirect evidences. The rescued palatal fusion in Tgf-β3$^{-/-}$/K14-Smad2 mice, however, never proceeded to the junction of primary and secondary palates and the most posterior border of the soft palate, despite phospho-SMAD2 expression in these regions at the same level as in the middle portion of the secondary palate. The K14-Smad2 transgene was unable to restore all the functional outcomes of TGF-β3. This may indicate an anterior–posterior patterning in the palatal shelves with respect to TGF-β3 signaling and the mechanism of secondary palatal fusion.
© 2004 Elsevier Inc. All rights reserved.

Keywords: TGF-β3; Smad2; Keratin 14; Overexpression; Mouse; Cleft palate; Palatal fusion; Medial edge epithelium; Epithelial–mesenchymal transformation; Rescue

Introduction

Transforming growth factor (TGF)-β3 has been shown to play an important role in the events regulating the disappearance of the medial edge epithelium (MEE) during palatal fusion. Tgf-β3-null mutant (Tgf-β3$^{-/-}$) mice have a cleft palate that is the principal developmental defect visualized at birth in these mice (Kaartinen et al., 1995; Proetzel et al., 1995). Previous studies suggested that all Tgf-β3$^{-/-}$ mice exhibited cleft palate, however, the severity of the cleft varied between different mouse genetic backgrounds (Kaartinen et al., 1995; Koo et al., 2001; Proetzel et al., 1995). The cleft palate phenotype was most severe on the C57BL/6 back-

ground, in which about 50% of Tgf-β3$^{-/-}$ mice had a complete cleft while the remainder had partial clefts. Thus, Tgf-β3 knockout mice with a C57BL/6 background have been most often used in the analysis of secondary palate development (Blavier et al., 2001; Cui et al., 2003; Gato et al., 2002; Kaartinen et al., 1997; Martínez-Álvarez et al., 2000a,b; Taya et al., 1999).

The TGF-β family initiates signaling by triggering a phosphorylation cascade initiated by TGF-β receptors (TβRs) and members of the SMAD family. SMAD2/3 are phosphorylated by the TβR complex and then bind to SMAD4. The SMAD2/3–SMAD4 complex is translocated into the nucleus to participate in an alteration of gene expression (Heldin et al., 1997; Massagué, 1998). Previously, we examined the distribution pattern of TGF-β3, TβRs, and SMADs in the developing palate to understand the restriction of TGF-β3 signaling to the MEE in a

---

developmental stage specific manner (Cui and Shuler, 2000; Cui et al., 1998, 2003). We found that the expression pattern of TGF-β3, receptors TβR-I and-II, and SMAD2 were consistent. They were localized predominantly to the epithelium covering the palatal shelves, which included the palatal oral epithelium, palatal nasal epithelium, and MEE before and during palatal shelf contact in the midline (Cui and Shuler, 2000; Cui et al., 1998, 2003). Expression of TβR-III (betaglycan) and SMAD2 phosphorylation, however, was shown to be spatially restricted to the MEE and temporally correlated with the disappearance of the MEE during palatal fusion. Both TβR-III and phospho-SMAD2 were present in the MEE immediately prior to palatal shelf contact in the midline, and both retained an exclusive distribution in the MEE as fusion progressed (Cui and Shuler, 2000; Cui et al., 2003). The results suggested that TGF-β3 exerted its developmental role in palatal fusion in an autocrine manner through TβR-I and-II binding. The role of TβR-III was hypothesized to localize and mediate TGF-β3's effect on MEE by specific presentation in the MEE. As a consequence, SMAD2 phosphorylation was spatially restricted to the MEE. In Tgf-β3$^{-/-}$ mice, the palate had a typical distribution of TGF-β1 and-β2 ligands and receptors (Taya et al., 1999), however, no phosphorylated SMAD2 was identified in the MEE (Cui et al., 2003). The absence of phospho-SMAD2 was correlated with the persistence of the MEE and failure of palatal fusion in Tgf-β3$^{-/-}$ mice. The results suggested that TGF-β3 was required for initiating and maintaining SMAD2 phosphorylation in the MEE that was required for alterations in gene expression necessary to complete palatal fusion. The endogenous TGF-β1 and-β2 alone were unable to trigger the SMAD2 phosphorylation to rescue the MEE fate in vivo (Cui et al., 2003).

One strategy hypothesized to rescue the cleft palate phenotype in Tgf-β3-deficient mice was to achieve MEE-specific overexpression of Smad2 in the Tgf-β3$^{-/-}$ MEE. The Keratin 14 promoter driving Smad2 expression (K14-Smad2) in the MEE appeared to be capable of providing overexpression of Smad2 in the MEE. It has been shown that in K14-Smad2 transgenic mice there was overexpression of Smad2 mRNA and translation of the Smad2 mRNA into protein in Keratin 14-synthesizing epidermal cells (Ito et al., 2001). The overexpressed SMAD2 was phosphorylated and translocated into the nucleus, regulated TGF-β target gene expression, and triggered a positive feedback on TGF-β signaling in a pathway-specific manner (Ito et al., 2001). Keratin 14 has been shown to have high levels of expression in the MEE in embryonic palatal epithelial sheet cultured in vitro by immunohistochemistry (Carette et al., 1991). We thus hypothesized that overexpression of K14-Smad2 in the MEE of Tgf-β3-null mutants could rescue the cleft palate phenotype via a positive induction of the TGF-β signaling pathway. This approach would bypass an initial requirement for TGF-β3 ligand binding to the TGF-β receptors to initiate SMAD2 phosphorylation in the MEE.

The goal of this study was to attempt rescue of the cleft palate phenotype in the Tgf-β3$^{-/-}$ mice by overexpression of a Smad2 transgene in the MEE following mating Tgf-β3 heterozygous mice (Tgf-β3^{tm1Doe}) with mice carrying the Smad2 transgene-driven by the K14 promoter (K14-Smad2).

Materials and methods

Animals and genotyping

Tgf-β3^{tm1Doe} heterozygous mice (Tgf-β3$^{+/-}$) had been backcrossed for at least 12 generations onto the C57BL/6J background (Jackson Laboratories, Bar Harbor, ME). Tgf-β3$^{+/-}$ mice were bred to generate Tgf-β3$^{-/-}$ newborns to determine the palatal phenotype in highly backcrossed C57BL/6J genetic background of the Tgf-β3 knockout mice.

K14-Smad2 transgenic mice were generously provided by Dr. Yang Chai (Ito et al., 2001). Tgf-β3^{tm1Doe} heterozygous mice were mated with K14-Smad2 mice to generate a Tgf-β3$^{+/-}$/K14-Smad2 line, which was then crossmated to produce Tgf-β3$^{-/-}$/K14-Smad2 newborns to determine whether MEE-directed overexpression of a Smad2 transgene could rescue the cleft palate phenotype in Tgf-β3$^{-/-}$ mice.

The genotype of the mice was determined by PCR using genomic DNA extracted from tail biopsies of either adults or newborns. Primers used to detect the Tgf-β3 knockout were located in intron 5 and intron 6 of Tgf-β3 (Taya et al., 1999). Primers used to detect the K14-Smad2 transgene were designed to be specific for the K14 region (Ito et al., 2001).

Fetuses obtained from timed pregnant C57BL/6J mice were used to immunolocalize phospho-SMAD2 in the developing palate. Fetuses were obtained between embryonic (E) days 14.5 and 15.5 as previously described (Cui et al., 1998).

Assessment of palatal fusion

Newborn mice were collected immediately post partum. Neonatal heads were immediately dissected. The jaw and tongue were removed to evaluate both hard and soft palate by direct observation with a dissecting microscope. Palatal fusion was scored on a 0 to 13 point scale. The criteria for this scale are as follows. (i) The nine rugae were used to establish landmarks to locate specific fusion positions on the palatal shelves (Sakamoto et al., 1991). The starting and ending fusion points were documented by the position of ruga. The total number of rugae fused was scored. For example, if partial fusion starts at the 3rd ruga and ends at the 5th ruga, the score is 3. There are a total of 9 points equaling fusion at all 9 rugae that can be assigned for fusion of the secondary hard palate. (ii) The pterygoid

plate was used as a landmark to locate specific fusion positions on the soft palate. Pterygoid plate can be observed through the thin soft palatal mucous with a dissecting microscope. Each 1/3 of pterygoid plate length represents 1 point. There are a total of 3 points that can be assigned for complete fusion of the soft palate. (iii) Fusion of primary palate and secondary palate is assigned 1 point (Fig. 1). Thus, a score of 0 represents complete cleft palate, whereas a score of 13 represents complete palatal fusion. All palatal fusion images were recorded by digital camera for duplicate assessments prior to processing the tissue for histological analysis.

Histological analysis

All neonatal heads were fixed in 10% buffered formalin after they were assessed for palatal fusion. To confirm palatal fusion at the histologic level, Tgf-β3$^{-/-}$/K14-Smad2 neonatal heads were embedded in paraffin. Coronal sections (7 μm) were prepared serially from anterior to posterior and processed for hematoxylin and eosin staining. Palatal fusion was confirmed if there was an absence of epithelium retained in the midline of palate.

Immunostaining

The embryonic heads were fixed in 4% paraformalde-hyde-PBS at 4°C, followed by routine procedures for embedding in paraffin. Coronal or sagittal sections (6 μm) were mounted in serial order on poly-L-lysine-coated slides. The specific anti-phospho-SMAD2 (rabbit polyclonal IgG) antibody was purchased from the Cell Signaling Technology, Inc. (Beverly, MA). A Histostain kit (Zymed Laboratories, Inc., South San Francisco, CA) was used to carry out the immunohistochemical analysis as previously described (Cui et al., 1998).

Western blot analysis

To determine the levels of SMAD2 expression in the Tgf-β3$^{-/-}$/K14-Smad2 mice, skin tissues were dissected from the neonatal body and lysed with a boiling solution containing SDS and 0.1 M DTT (Ito et al., 2001). One hundred-microgram total protein per specimen was loaded in each well on a 12% polyacrylamide gel. Electrophoresis was carried out in a modular mini-Protean II electrophoresis system (Bio-Rad, Hercules, CA). Protein was then transferred to a Millipore Immobilon-P membrane using a Bio-Rad minitransblot electrophoretic transfer cell. The subsequent Western blot was performed by using a chemiluminescent Western blot kit (Boehringer Mannheim, Indianapolis, IN). The primary antibody (mouse monoclonal IgG) against SMAD2 (BD Transduction Laboratories, San Diego, CA) or phospho-SMAD2 (Cell Signaling Technology, Inc.) was incubated with the membrane overnight at 4°C. The results were captured by Kodak X-Omat AR film and measured by a computer image analysis program. Correlation between phospho-SMAD2 protein level and palate fusion was analyzed statistically by the Spearman non-parametric method. The primary antibody (goat polyclonal IgG) against β-ACTIN (Santa Cruz Biotechnology, Inc., Santa Cruz, CA) was used as an internal control.

Results

K14-Smad2 transgene rescues cleft palate in Tgf-β3$^{-/-}$ mice

The hallmark of Tgf-β3$^{-/-}$ mice is that they display either complete cleft palate or severe partial cleft palate at birth. The Tgf-β3$^{-/-}$ pups die within 24 h of birth as they could not successfully suckle (Kaartinen et al., 1995;
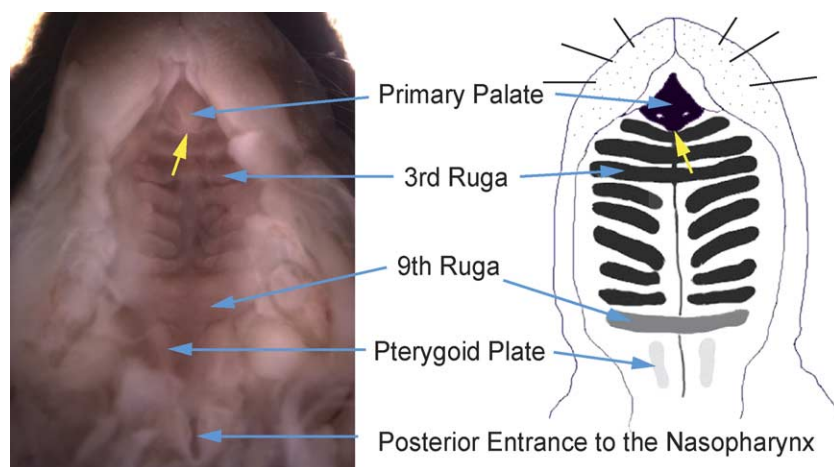

Fig. 1. Image (left) and schematic diagram (right) of the palate of neonatal mouse at P0. The nine rugae are used to establish landmarks to locate specific fusion positions on the hard palate. Rugae are numbered in anterioposterior sequence. The pterygoid plate is used as a landmark to locate specific fusion positions on the soft palate. Pterygoid plate can be observed through the thin soft palatal mucous (image on the left). Arrow (yellow color) indicates the site of fusion of primary and secondary palates.

Proetzel et al., 1995). The aim of this study was to determine if rescue of the cleft palate phenotype could be achieved by overexpressing Smad2 in the MEE using the K14 promoter to direct Smad2 expression. A Tgf-β3$^{+/-}$/K14-Smad2 line was generated by mating Tgf-β3$^{+/-}$ mice (Tgf-β3^{tm1Doe}) with K14-Smad2 mice. The Tgf-β3$^{+/-}$/K14-Smad2 mice retained the phenotype of the K14-Smad2 transgenic mice including features such as delayed hair growth, underdeveloped ears and shorter tails (Ito et al., 2001), but had no abnormality of the palate. Tgf-β3$^{+/-}$/K14-Smad2 mice were crossmated to generate Tgf-β3$^{-/-}$/K14-Smad2 pups. Of 21 Tgf-β3$^{-/-}$/K14-Smad2 newborns examined, all exhibited palatal fusion in the secondary hard palate. The breeding line that generated the largest number of offspring for analysis is specifically reported in greater detail in the following section. This breeding pair produced sufficient offspring for statistical analysis with a consistent genetic background.

A total of 50 offspring from Tgf-β3$^{+/-}$/K14-Smad2 crosses from one breeding pair were collected soon after birth. The genotypes of all specimens were determined by PCR. In particular, 11 specimens were Tgf-β3$^{-/-}$, of which 6 were also positive for the K14-Smad2 transgene (Tgf-β3$^{-/-}$/K14-Smad2) while the remaining Tgf-β3$^{-/-}$ newborns were negative for the K14-Smad2 transgene (Tgf-β3$^{-/-}$). All Tgf-β3$^{-/-}$/K14-Smad2 and 4 of 5 Tgf-β3$^{-/-}$ pups were alive at the time of collection. One Tgf-β3$^{-/-}$ pup was found dead.

Tgf-β3$^{-/-}$/K14-Smad2 and Tgf-β3$^{-/-}$ newborns were assessed for palate fusion by direct observation with a dissecting microscope. As shown in Table 1, 4 of 5 Tgf-β3$^{-/-}$ animals had complete cleft palate (Fig. 2A). One Tgf-β3$^{-/-}$ palate had a partial cleft with limited fusion between

Table 1
Palatal fusion assessment

| Genotype	Sample no.	Fusion score	Description of palatal fusion
Tgf-β3$^{-/-}$	a	0	No fusion (complete cleft palate)
	b	0	No fusion (complete cleft palate)
	c	0	No fusion (complete cleft palate)
	d	0	No fusion (complete cleft palate)
	e	4	Fusion between 3rd and 6th ruga
Tgf-β3$^{-/-}$/ K14-Smad2	f	6	Fusion between 2nd and 7th ruga
	g	7	Fusion between 2nd and 8th ruga
	h	8	Fusion between 1st and 8th ruga
	i	10	Fusion between 1st ruga and anterior 1/3 of soft palate
	j	11	Fusion between 1st ruga and middle 1/3 of soft palate
	k	11	Fusion between 1st ruga and middle 1/3 of soft palate
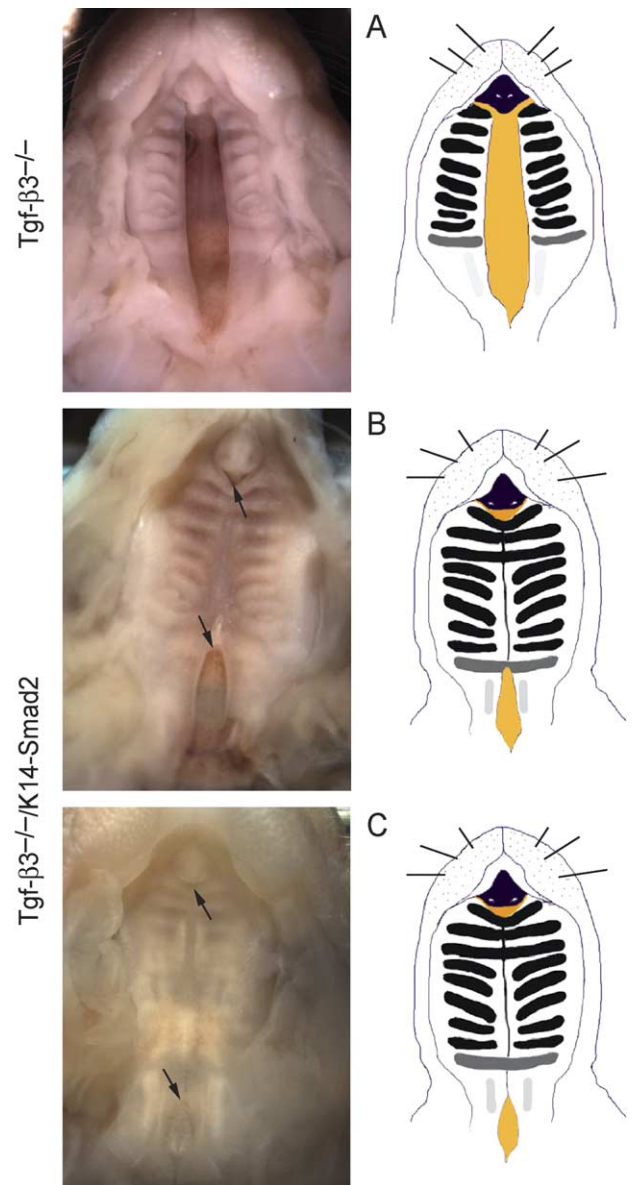
Fig. 2. Images (left) and schematic diagrams (right) of the palate of neonatal mice at P0 to demonstrate various cleft palate/palatal fusion phenotypes. (A) Tgf-β3$^{-/-}$ newborn: complete cleft palate. (B and C) Tgf-β3$^{-/-}$/K14-Smad2 newborns. (B) Rescue of palatal fusion (between arrows) is limited between the 1st and 8th ruga of the secondary hard palate. The posterior secondary palate remains unfused from the posterior border of the 9th ruga to the entire soft palate. An anterior cleft is present at the junction between the primary and secondary palate. (C) Rescue of palatal fusion (between arrows) proceeds for the entire secondary hard palate and anterior portion of the soft palate. The posterior soft palate, however, remains unfused. An anterior cleft is present at the junction between the primary and secondary palate. Arrow points anterior or posterior cleft.

the 3rd and 6th ruga. In Tgf-β3$^{-/-}$/K14-Smad2 group, none of the newborns had complete cleft palate. Instead, they all exhibited palatal fusion with a minimum of 6 rugae range (Table 1). Three of 6 Tgf-β3$^{-/-}$/K14-Smad2 newborns had palatal fusion that proceeded for the entire secondary hard palate and anterior portion of the soft palate. The posterior soft palate, however, remained unfused (Fig. 2C). An

anterior cleft was also present at point of junction between the primary and secondary palate in Tgf-β3$^{-/-}$/K14-Smad2 mice (Figs. 2B and C).

Palatal fusion of Tgf-β3$^{-/-}$/K14-Smad2 neonatal mice was verified microscopically by examining serial histologic sections of the secondary palates. The results showed that in sections from the 1st ruga region, the opposing palatal shelves had not contacted in the midline either between each other or between the palatal shelves and the nasal septum. The palatal epithelium was intact (Fig. 3A). Palatal fusion is normally complete at E16. No epithelium is identified in the midline of secondary palate or at the junctions of the primary and secondary palates after E16 (Kaufman, 1992). The failure of palatal shelf fusion in the midline in the 1st ruga region in Tgf-β3$^{-/-}$/K14-Smad2 specimens after birth
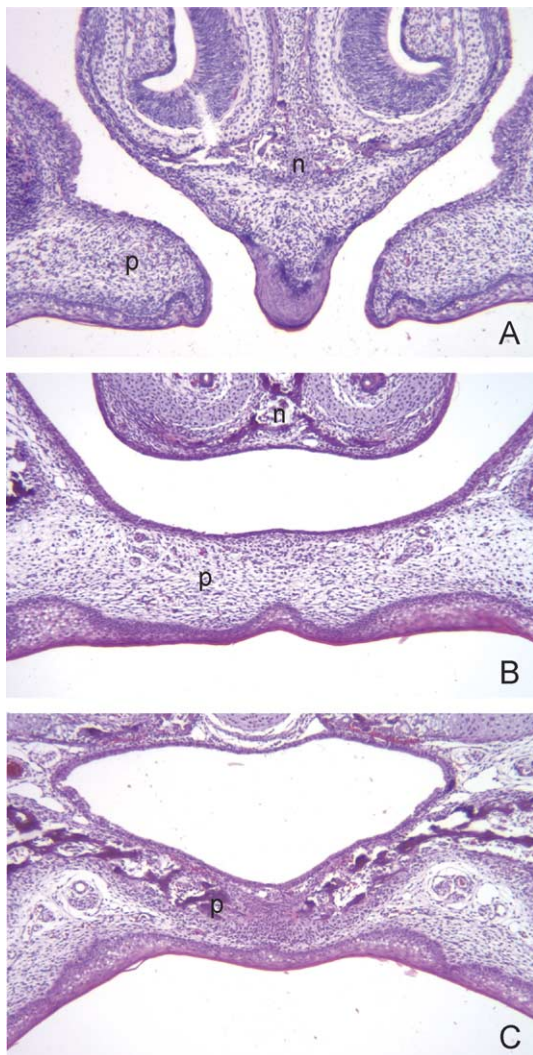

Fig. 3. Histology of partially rescued Tgf-β3$^{-/-}$/K14-Smad2 palate at P0 (H and E staining). (A) The opposing palatal shelves have no contact in the midline either between each other or between the palatal shelves and the nasal septum in the first ruga region. (B and C) The secondary palate is fused with mesenchymal confluence and no epithelial midline seam. (B) Anterior secondary hard palate. (C) Posterior secondary hard palate. n: nasal septum. p: palatal shelf.

is consistent with the failure of fusion between the primary and secondary palate observed with a dissecting microscope. The remainder of the secondary hard palate was completely fused with mesenchymal confluence and no epithelial midline seam (Figs. 3B and C). The absence of epithelium in the midline of the intact secondary palate confirms completion of secondary hard palatal fusion.

Palatal fusion outcomes correlate with the phospho-SMAD2 level

To determine if the improved palatal fusion in Tgf-β3$^{-/-}$/K14-Smad2 newborns resulted from overexpression of the Smad2 transgene, it was important to examine SMAD2 and phospho-SMAD2 expression at the protein level and correlate the protein level with the palate fusion outcomes. Neonatal mice have passed the developmental stage that demonstrated SMAD2 phosphorylation occurred in the MEE during palatal fusion. Therefore, we used neonatal epidermis as an alternative Keratin 14-synthesizing tissue to demonstrate the SMAD2/phospho-SMAD2 level in Tgf-β3$^{-/-}$/K14-Smad2 individuals by Western blot analysis (Ito et al., 2001). As shown in Fig. 4A, Tgf-β3$^{-/-}$ mice without the K14-Smad2 transgene had little SMAD2 and very low levels of phospho-SMAD2 production (Fig. 4A: a, b, c, d, e). Correspondingly, the fusion scores were low (0–4 points) (Fig. 4B). The Tgf-β3$^{-/-}$/K14-Smad2 counterparts, however, demonstrate higher levels of both SMAD2 and phospho-SMAD2 in 4 of 6 specimens (Fig. 4A: g, i, j, k). The specimens with the most prominent phospho-SMAD2 production (Fig. 4A: j, k) had the highest palatal fusion score (11 points) (Fig. 4B). Correlation between the phospho-SMAD2 level (normalized by the β-ACTIN protein level) and the palatal fusion outcomes was further analyzed statistically by the Spearman non-parametric method. The result showed that the ranked palatal fusion score had a statistically significant correlation with the normalized phospho-SMAD2 quantities ($P < 0.05$). The result supported the hypothesis that the palatal fusion outcome was correlated with the phospho-SMAD2 level. The rescue of palatal fusion in Tgf-β3 null mutants could be attributed to the elevated phospho-SMAD2 level associated with the SMAD2 overexpression generated by the K14-Smad2 transgene.

Phospho-SMAD2 is expressed in all regions of anticipated palatal fusion in K14-Smad2 transgenic mice

K14-Smad2 transgene rescued cleft palate phenotype of Tgf-β3-null mice. The rescue of palatal fusion was limited to the secondary hard palate and the anterior 2/3 of the soft palate (Table 1). Palatal fusion did not occur either at the posterior soft palatal shelf region or between the primary and secondary palates (Fig. 2C). A previous study has suggested that heterogeneity existed along the anterioposterior axis of the developing palate (Zhang et al., 2002). Our conclusion regarding the transgene directed Smad2 over-
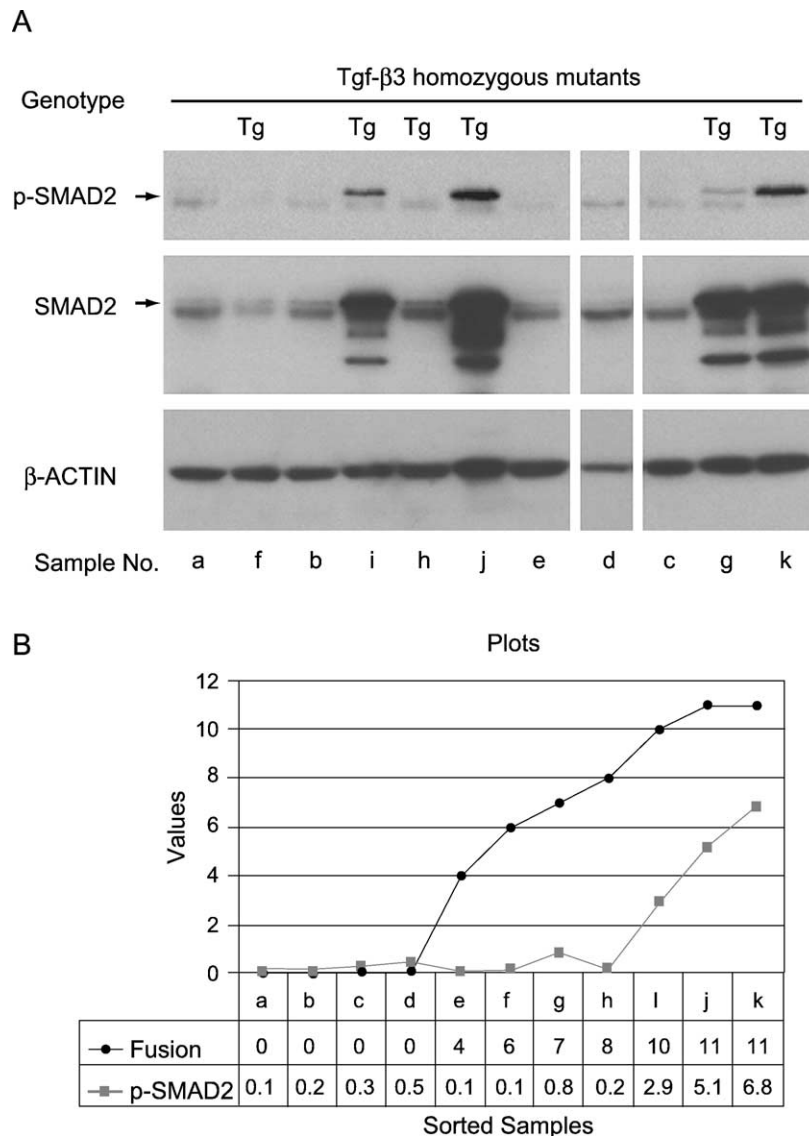
Fig. 4. Correlation of SMAD2/phospho-SMAD2 expression level with the palatal fusion outcomes. (A) Western blot analysis of expression of SMAD2 and phospho-SMAD2 in epidermis in Tgf-β3$^{-/-}$ mice with or without the K14-Smad2 transgene. (B) Plots of values of phospho-SMAD2 measurement (normalized by the β-ACTIN level) and palatal fusion score versus sorted 11 Tgf-β3$^{-/-}$ samples with or without the K14-Smad2 transgene.

expression was generated from study of epidermal cells and did not analyze palatal tissues. Therefore, the expression of phospho-SMAD2 in the palate in K14-Smad2 mice was analyzed by immunohistochemistry to determine whether phospho-SMAD2 was expressed at all positions along the palatal shelf required for palatal fusion. Special attention was paid to the anterior and posterior extremities of the secondary palate, regions not rescued by Smad2 overexpression directed by K14 promoter.

Palatal fusion initially occurs in the middle region of the palatal shelves at E14.5. The opposing palatal shelves contact in the midline and form an epithelial seam. Both anterior and posterior to this site, the shelves have yet to become in contact (Kaufman, 1992). At this stage, phospho-SMAD2 expression was exclusively localized to the MEE and the palatal oral and nasal epithelium immediate adjacent

to the midline seam (Figs. 5A–C). The nasal epithelium at the base of nasal septum in the region of presumptive fusion was also positive for phospho-SMAD2 staining (Fig. 5A). The spatially restricted expression pattern of phospho-SMAD2 in the palate in K14-Smad2 transgenic mice was consistent with previous study on the wild-type animal (Cui et al., 2003). At the identical concentration of anti-phospho-SMAD2 antibody, the control animals did not have detectable phospho-SMAD2 in the MEE (Figs. 5D and E). The experimental conditions were controlled so that the positive stains could be well detected in the MEE of the transgenic specimens, but not in the tissues without K14-Smad2 transgene as demonstrated in Fig. 5.

By E15.5, the palatal shelves have fused with each other, and with the inferior border of the nasal septum. The primary palate has begun to join the secondary palate and at
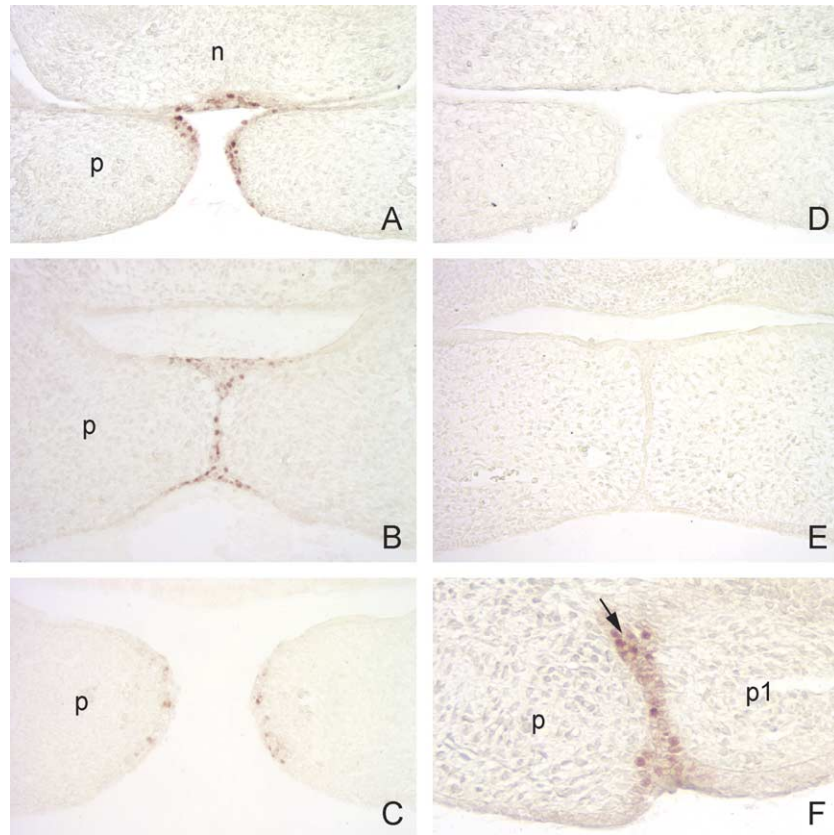
Fig. 5. Immunolocalization of phospho-SMAD2 in the palate in K14-Smad2 transgenic mice to demonstrate phospho-SMAD2 in all regions of palate. (A–E) E14.5, coronal section, 20×. (A–C) Transgenic tissues. (D and E) Non-transgenic tissues. (F) E15.5, sagittal section, 40×, transgenic tissue. (A–C) E14.5. Phospho-SMAD2 expression is exclusively localized to the MEE and the palatal oral and nasal epithelium adjacent to the midline seam of the palate. This occurs both with respect to the in-fusion region (B) and the presumptive fusion regions that include anterior palate (A) and the posterior extremity of the palate (C). The nasal epithelium at the base of nasal septum to be fused with palatal shelves is also positive with phospho-SMAD2 expression (A). (D and E) E14.5. Phospho-SMAD2 expression is not detectable in either MEE or nasal epithelium in the littermate controls. (F) E15.5. Phospho-SMAD2 expression retains the pattern observed in the E14.5 palate that is correlated with the formation and disruption of epithelial seams at the sites of fusion. Phospho-SMAD2 presents in the region between the primary palate and the anterior extremity of the secondary palate (arrow). n: nasal septum. p: secondary palate. p1: primary palate.

this point, phospho-SMAD2 was highly expressed in the fusion region (Fig. 5F). Phospho-SMAD2 was present in all regions that fuse in normal palatogenesis. The results confirmed that K14 promoter was able to direct Smad2 gene overexpression and subsequent phosphorylation in the MEE along the anterioposterior axis of the entire palate immediately before and during palatal fusion. Failure of rescue of the cleft palate phenotype in the anterior and posterior extremities of the palate in the Tgf-$\beta3^{-/-}$/K14-Smad2 animals was not due to heterogeneity of Smad2 expression directed by K14 promoter.

High occurrence of complete cleft palate in Tgf-β3^{tm1Doe} homozygous null mutants

An important control for these rescue experiments was to determine the palatal phenotype in highly backcrossed C57BL/6J genetic background of the Tgf-β3 null mutant mice. Previously, this had not been determined (Kaartinen et al., 1995; Proetzel et al., 1995) and it was critical to know the background of palatal fusion in this mouse line. We

examined Tgf-β3^{tm1Doe} offspring at P0 to characterize the developmental pattern of the palatal tissues. A total of 335 pups were collected immediately post partum. The expected mendelian ratio of wild type, heterozygous and homozygous offspring was obtained (24.2% Tgf-β3$^{+/+}$, 51.6% Tgf-β3$^{+/-}$ and 24.2% Tgf-β3$^{-/-}$ pups), indicating little prenatal mortality. The result is consistent with previous reports (Kaartinen et al., 1995; Proetzel et al., 1995).

Palatal fusion at P0 was evaluated by direct observation with a dissecting microscope and histologic analysis of serial sections. The results showed that 100% of Tgf-β3$^{-/-}$ newborns ($n = 81$) had cleft secondary palate, 91.4% had a complete cleft (74/81) while 8.6% partial cleft (7/81) (Table 2). In complete clefts, the bilateral palatal shelves were separated from each other and the vomer was exposed to the oral cavity. In partial cleft palate, fusion was limited to the region between the 2nd and 5th ruga (Fig. 6A). Histological examination confirmed that no epithelium was retained in the midline fusion region. High penetrance of complete cleft palate occurred in the highly backcrossed Tgf-β3 null mutant mice with the C57BL/6J genetic background. The

Table 2
Occurrence of cleft palate in Tgf-β3[tm1Doe] newborns

Genotype	Total sample no.	Complete cleft		Partial palate		Anterior cleft	
		No.	Ratio (%)	No.	Ratio (%)	No.	Ratio (%)
Tgf-β3$^{-/-}$	81	74	91.4	7	8.6	N/A	N/A
Tgf-β3$^{+/-}$	171	0	0	0	0	15	8.8
Tgf-β3$^{+/+}$	80	0	0	0	0	2	2.5

results confirmed the crucial role of TGF-β3 in the regulation of palatal fusion and provided valuable background evidence in the Tgf-β3[tm1Doe] knockout mice for analysis of genetic rescue of the cleft phenotype.

It was noted that 8.8% of the Tgf-β3$^{+/-}$ newborns (15/171) and 2.5% of the Tgf-β3$^{+/+}$ newborns (2/80) demonstrated a failure of fusion between the primary and secondary palates, namely anterior cleft (Fig. 6B, Table 2) (χ^2 test, $0.10 > P > 0.05$). This type of cleft defect had not been previously reported in any Tgf-β3$^{+/-}$ or Tgf-β3$^{+/+}$ offspring (Kaartinen et al., 1995; Proetzel et al., 1995). The phenotype of the anterior cleft in Tgf-β3[tm1Doe] newborns (Fig. 6B) was identical to the observation in Tgf-β3$^{-/-}$/K14-Smad2-rescued newborns (Fig. 2C). Neither complete cleft nor partial cleft secondary palate was detected in either Tgf-β3$^{+/-}$ ($n = 171$) or Tgf-β3$^{+/+}$($n = 80$) newborns (Table 2). These detailed analyses provide a solid background for evaluating the K14-Smad2 rescue of the Tgf-β3$^{-/-}$ cleft palate and demonstrate that overexpression does rescue the clefting.

Discussion

The mammalian palate is formed by the union of three elements: the primary palate from the frontonasal process and the two lateral maxillary palatal shelves from the first branchial arch that will form the secondary palate. Palatal

Fig. 6. Images of the palate of neonatal Tgf-β3[tm1Doe] mice at P0 to demonstrate various cleft palate phenotypes. (A) Tgf-β3$^{-/-}$: partial cleft palate. Palatal fusion (between arrows) is limited between the 2nd and 5th ruga. (B) Tgf-β3$^{+/-}$: an anterior cleft is present at the junction between the primary and secondary palate (arrowhead).

fusion involves three events. Laterally, the palatal shelves of the maxillae (the future secondary palate) fuse across the midline to form the roof of the oropharynx. Superiorly, the palatal shelves in the midline fuse with the inferior border of the nasal septum. In the anterior region, the anteromedial borders of the palatal shelves fuse with the primary palate (Kaufman, 1992). Palatal fusion is completed within a very short period of time. During murine palatogenesis, palatal fusion starts at E14.5 in the middle region of the shelves (opposite the second to fourth pairs of rugae) and progresses toward the posterior. Soon after, the superior and anterior aspects of fusion take place. By E15.5, the fusion process is virtually complete. The final region to close at about E16 is close to the site where the primary and secondary palates meet in the region of the incisive canal. Meanwhile, the rugae associated with the mucosa on the oral surface of the palate become more prominent at E16. A total of nine rugae of various sizes are seen in the mouse (Kaufman, 1992; Sakamoto et al., 1991; Shuler, 1995). Our scoring system used to assess palatal fusion in the mice was established based on the sequential events of palatal fusion.

Rescue of the cleft palate phenotype in the Tgf-β3-null genetic background was attempted by a transgenic approach conducted by cross-breeding Tgf-β3$^{+/-}$ mice (Tgf-β3[tm1Doe]) with K14-Smad2 transgenic mice to produce Tgf-β3$^{-/-}$/K14-Smad2 offspring. The results showed that the Tgf-β3$^{-/-}$ offspring without Smad2 transgene retained the high incidence of complete cleft palate as seen in the detailed analysis of the cleft palate phenotype in the Tgf-β3[tm1Doe] homozygous mutants. In contrast, the Tgf-β3$^{-/-}$ mice with the Smad2 transgene driven by K14 promoter demonstrated a rescue of palatal fusion. Two additional sets of results indicated that success of rescue in Tgf-β3$^{-/-}$/K14-Smad2 mice was dependent on an elevated level of phospho-SMAD2 in the MEE. First, the Tgf-β3$^{-/-}$/K14-Smad2 individuals that exhibited near complete palatal fusion had the highest phospho-SMAD2 level in the Keratin 14-synthesizing epidermis. Second, examination of E14.5-15.5 embryonic mice demonstrated phospho-SMAD2 in the MEE in K14-Smad2 mice. The non-K14-Smad2 transgenic control littermates did not show phospho-SMAD2 in the MEE under the same experimental condition. The results indicate that rescue of palatal fusion in Tgf-β3-null mutants could be achieved through the directed overexpression of SMAD2 in the MEE.

Previous research demonstrated that the overexpressed SMAD2 in K14-Smad2 transgenic mice resulted in an elevation of the endogenous TGF-β1 level, but did not
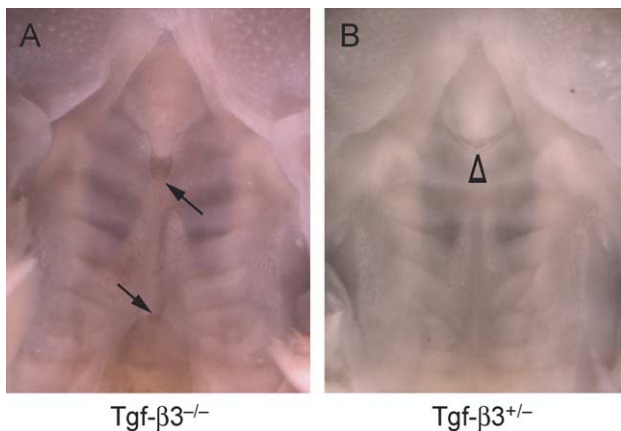
affect either the TGF-β2, TGF-β3, or Smad3 expression levels (Ito et al., 2001). Correspondingly, overexpression of Smad2 in the Tgf-β3$^{-/-}$ genetic background should increase TGF-β1 expression and consequently TGF-β1 signaling. It is possible that TGF-β1 functions to activate SMAD2/phospho-SMAD2 and participates in the rescue of the palatal fusion. Overexpression of Smad2 was thus able to bypass an initial requirement for TGF-β3 ligand binding to the TGF-β receptors to initiate SMAD2 phosphorylation in the MEE.

It has been reported that in Tgf-β3$^{-/-}$ mice there were alterations with regard to the adhesion molecules in the MEE (Tudela et al., 2002). In Tgf-β3$^{+/+}$ palates, the presence of associated E-cadherin, α- and β-catenin, and β-actin were present circumferentially in the basal cells and basolaterally in the superficial cells in the pre-adhesion MEE. In Tgf-β3$^{-/-}$ palate tissues, E-cadherin and α-catenin were also located to apical regions of the MEE cells and β-catenin was irregularly distributed in the cytoplasm. The abnormal distribution of E-cadherin and E-cadherin associated molecules in the Tgf-β3$^{-/-}$ MEE was correlated with defect in the adhesion between opposing MEE and subsequent failure of palatal fusion (Tudela et al., 2002). A relationship between TGF-β1 signaling and adhesion molecules has also been investigated (Miettinen et al., 1994; Piek et al., 1999). TGF-β1 was able to induce epithelial–mesenchymal transdifferentiation of a murine mammary epithelial cell line NMuMG that was associated with a change in cell morphology correlated with downregulation and relocalization of E-cadherin and β-catenin, and SMAD2 phosphorylation with nuclear translocation (Miettinen et al., 1994; Piek et al., 1999). These results suggest that TGF-β1-inducted SMAD2 phosphorylation lead to changes in adhesion during morphologic transdifferentiation of NMuMG cells. Improved palatal fusion in the Tgf-β3$^{-/-}$/K14-Smad2 mice may be linked to the downregulation/relocalization of E-cadherin and associated molecules to the apical surface of the Tgf-β3$^{-/-}$ MEE, however, these studies were not the subject of the current project.

In the present study, the rescue never proceeded either to the junction of primary and secondary palates or the most posterior border of the soft palate, despite phospho-SMAD2 presence in these regions at the same level as in the middle portion of the secondary palate. This result suggests there may be anterior–posterior patterning in the palatal shelves and that additional mechanisms may be active at the most anterior and posterior locations. TGF-β3 signaling may accomplish more than just activation of SMAD2 to result in the complete fusion of the palate in the most anterior and posterior regions. The result further supports the notion that TGF-β3 is a key initiator of the onset of the MEE disappearance during palatal fusion (Cui et al., 2003) and provides evidence that regional mechanisms might differ between anterior and posterior segments of the palate.

Previous attempts to rescue the Tgf-β3$^{-/-}$ cleft palate phenotype were successful by supplement with additional recombinant TGF-β3 in vitro (Kaartinen et al., 1997; Taya et al., 1999). However, the rescues of palatal fusion were assessed only for the secondary palate. The fusion between the primary palate and secondary palate was not assessed as the organ culture system used in these studies excluded the primary palate in the culture system. The most anterior and posterior portions of the secondary palate were also not assessed for palatal fusion due to the culture approach. The conclusions reached from the rescue of palatal fusion in the null mutants in vitro organ culture may be limited due to the methodology.

In summary, the cleft palate phenotype in Tgf-β3$^{-/-}$ mice could be rescued in vivo by overexpression of a Smad2 transgene in the Keratin 14-synthesizing MEE cells following mating Tgf-β3^{tm1Doe} heterozygous mice with K14-Smad2 transgenic mice. Success of the rescue could be attributed to the elevated phospho-SMAD2 level in the MEE. However, MEE-directed overexpression of Smad2 in Tgf-β3 null mutants was not able to restore all the functional outcomes of TGF-β3 signaling, since in all cases, minor incomplete palatal fusion persisted at both the junction of primary and secondary palates and in the most posterior soft palate. The result supports the notion that TGF-β3 is a key initiator of the onset of the MEE disappearance during palatal fusion (Cui et al., 2003) and provides evidence that regional mechanisms might differ between anterior and posterior segments of the palate. Tgf-β3$^{-/-}$ mice without the Smad2 transgene had a high incidence of complete cleft palate as seen in Tgf-β3^{tm1Doe} homozygous null mutant mice. This suggests that the genetically homogenous Tgf-β3^{tm1Doe} knockout model is valuable model to study TGF-β3 function in the regulation of the fate of the MEE during palatal fusion.

References

Blavier, L., Lazaryev, A., Groffen, J., Heisterkamp, N., DeClerck, Y.A., Kaartinen, V., 2001. TGF-beta3-induced palatogenesis requires matrix metalloproteinases. Mol. Biol. Cell 12, 1457–1466.

Carette, M.J., Lane, E.B., Ferguson, M.W., 1991. Differentiation of mouse embryonic palatal epithelium in culture: selective cytokeratin expression distinguishes between oral, medial edge and nasal epithelial cells. Differentiation 47, 149–161.

Cui, X.-M., Shuler, C.F., 2000. The TGF-β type III receptor is localized to the medial edge epithelium during palatal fusion. Int. J. Dev. Biol. 44, 397–402.

Cui, X.-M., Warburton, D., Zhao, J., Crowe, D.L., Shuler, C.F., 1998. Immunohistochemical localization of TGF-β type II receptor and TGF-β3 during palatogenesis in vivo and in vitro. Int. J. Dev. Biol. 42, 817–820.

Cui, X.-M., Chai, Y., Chen, J., Yamamoto, T., Ito, Y., Bringas, P., Shuler, C.F., 2003. TGF-beta3-dependent SMAD2 phosphorylation and inhibition of MEE proliferation during palatal fusion. Dev. Dyn. 227, 387–394.

Gato, A., Martinez, M.L., Tudela, C., Alonso, I., Moro, J.A., Formoso, M.A., Ferguson, M.W., Martinez-Álvarez, C., 2002. TGF-beta(3)-induced chondroitin sulphate proteoglycan mediates palatal shelf adhesion. Dev. Biol. 250, 393–405.

Heldin, C.H., Miyazono, K., ten Dijke, P., 1997. TGF-beta signaling from cell membrane to nucleus through SMAD proteins. Nature 390, 465–471 (Review).

Ito, Y., Sarkar, P., Mi, Q., Wu, N., Bringas Jr., P., Liu, Y., Reddy, S., Maxson, R., Deng, C., Chai, Y., 2001. Overexpression of Smad2 reveals its concerted action with Smad4 in regulating TGF-beta-mediated epidermal homeostasis. Dev. Biol. 236, 181–194.

Kaartinen, V., Voncken, J.W., Shuler, C.F., Warburton, D., Bu, D., Heisterkamp, N., Groffen, J., 1995. Abnormal lung development and cleft palate in mice lacking TGF-beta 3 indicates defects of epithelial–mesenchymal interaction. Nat. Genet. 11, 415–421.

Kaartinen, V., Cui, X.-M., Heisterkamp, N., Groffen, J., Shuler, C.F., 1997. Transforming growth factor-beta3 regulates transdifferentiation of medial edge epithelium during palatal fusion and associated degradation of the basement membrane. Dev. Dyn. 209, 255–260.

Kaufman, M.H., 1992. The Atlas of Mouse Development. Academic Press, San Diego.

Koo, S.-H., Cunningham, M.C., Arabshahi, B., Gruss, J.S., Grant, J.H., 2001. The Transforming growth factor-β3 knock-out mouse: an animal model for cleft palate. Plast. Reconstr. Surg. 108, 938–948.

Martínez-Álvarez, C., Bonelli, R., Tudela, C., Gato, A., Mena, J., O'Kane, S., Ferguson, M.W., 2000a. Bulging medial edge epithelial cells and palatal fusion. Int. J. Dev. Biol. 44, 331–335.

Martínez-Álvarez, C., Tudela, C., Pérez-Miguelsanz, J., O'Kane, S., Puerta, J., Ferguson, M.W., 2000b. Medial edge epithelial cell fate during palatal fusion. Dev. Biol. 220, 343–357.

Massagué, J., 1998. TGF-beta signal transduction. Annu. Rev. Biochem. 67, 753–791 (Review).

Miettinen, P.J., Ebner, R., Lopez, A.R., Derynck, R., 1994. TGF-β induced transdifferentiation of mammary epithelial cells to mesenchymal cells: involvement of type I receptors. J. Cell Biol. 127, 2021–2036.

Piek, E., Moustakas, A., Kurisaki, A., Heldin, C.H., ten Dijke, P., 1999. TGF-(beta) type I receptor/ALK-5 and Smad proteins mediate epithelial to mesenchymal transdifferentiation in NMuMG breast epithelial cells. J. Cell Sci. 112, 4557–4568.

Proetzel, G., Pawlowski, S.A., Wiles, M.V., Yin, M., Boivin, G.P., Howles, P.N., Ding, J., Ferguson, M.W.J., Doetschman, T., 1995. Transforming growth factor-beta 3 is required for secondary palate fusion. Nat. Genet. 11, 409–414.

Sakamoto, M.K., Nakamura, K., Handa, J., Kihara, T., Tanimura, T., 1991. Studies of variant palatal rugae in normal and corticosteroid-treated mouse embryos. Anat. Rec. 230, 121–130.

Shuler, C.F., 1995. Programmed cell death and cell transformation in craniofacial development. Crit. Rev. Oral Biol. Med. 6, 202–217 (Review).

Taya, Y., O'Kane, S., Ferguson, M.W., 1999. Pathogenesis of cleft palate in TGF-beta3 knockout mice. Development 126, 3869–3879.

Tudela, C., Formoso, M.A., Martínez, T., Pérez, R., Aparicio, M., Maestro, C., Del Río, A., Martínez, E., Ferguson, M., Martínez-Álvarez, C., 2002. TGF-beta3 is required for the adhesion and intercalation of medial edge epithelial cells during palate fusion. Int. J. Dev. Biol. 46, 333–336.

Zhang, Z., Song, Y., Zhao, X., Zhang, X., Fermin, C., Chen, Y., 2002. Rescue of cleft palate in Msx1-deficient mice by transgenic Bmp4 reveals a network of BMP and Shh signaling in the regulation of mammalian palatogenesis. Development 129, 4135–4146.